JACS
JOURNAL OF THE AMERICAN CHEMICAL SOCIETY
Communication
pubs.acs.org/JACS

Disappearance of Superconductivity in the Solid Solution between $(Ca_4Al_2O_6)(Fe_2As_2)$ and $(Ca_4Al_2O_6)(Fe_2P_2)$ Superconductors

Parasharam M. Shirage,* Kunihiro Kihou, Chul-Ho Lee, Nao Takeshita, Hiroshi Eisaki, and Akira Iyo*

National Institute of Advanced Industrial Science and Technology (AIST), Central-2, 1-1-1 Umezono, Tsukuba, Ibaraki-305 8568, Japan

ABSTRACT: The effect of alloying the two perovskite-type iron-based superconductors $(Ca_4Al_2O_6)(Fe_2As_2)$ and $(Ca_4Al_2O_6)(Fe_2P_2)$ was examined. While the two stoichiometric compounds possess relatively high T_c's of 28 and 17 K, respectively, their solid solutions of the form $(Ca_4Al_2O_6)(Fe_2(As_{1-x}P_x)_2)$ do not show superconductivity over a wide range from $x = 0.50$ to 0.95. The resultant phase diagram is thus completely different from those of other typical iron-based superconductors such as $BaFe_2(As,P)_2$ and LaFe(As,P)O, in which superconductivity shows up when P is substituted for As in the non-superconducting "parent" compounds. Notably, the solid solutions in the non-superconducting range exhibit resistivity anomalies at temperatures of 50−100 K. The behavior is reminiscent of the resistivity kink commonly observed in various non-superconducting parent compounds that signals the onset of antiferromagnetic/orthorhombic long-range order. The similarity suggests that the suppression of the superconductivity in the present case also has a magnetic and/or structural origin.

Besides exhibiting the second highest transition temperature (T_c) next to the cuprates, the newly discovered iron-based superconductors possess variety of interesting properties.[1] In particular, it is well-recognized that the superconducting order resides in proximity to the antiferromagnetic (AFM) order and that in most cases the superconductivity emerges by suppression of the AFM long-range order existing in the stoichiometric "parent" compounds. There are various ways to suppress this order. Typical examples are (1) doping of electrons/holes by chemical substitution, such as Co/K doping into $BaFe_2As_2$[2,3] and F doping or introduction of O deficiencies in *Ln*FeAsO (*Ln* = lanthanide),[4−6] and (2) application of physical/chemical pressure, such as the substitution of smaller P atoms at the As sites in $BaFe_2As_2$[7,8] and *Ln*FeAsO.[9,10]

On the other hand, there are several exceptional iron-based compounds that exhibit superconductivity without any doping or pressure. The most well-known material is LiFeAs, for which $T_c = 18$ K.[11] Another class of materials contain perovskite-based block layers, which are expressed as either $(AE_{n+1}TM_nO_{3n-1})(Fe_2Pn_2)$ [abbreviated as *TM*-$(n+1)n(3n-1)22(Pn)$] or $(AE_{n+2}TM_nO_{3n})(Fe_2Pn_2)$ [*TM*-$(n+2)n(3n)22(Pn)$], in which *AE* = Ca, Sr, Ba; *TM* = Mg, Al, Sc, Ti, V, Cr, etc.; and *Pn* = P, As.[12−19] A T_c of 47 K has been reported for $(Ca_4(Ti,Mg)_3O_8)(Fe_2As_2)$ [(Ti,Mg)-43822(As)], making this system the family with the second-highest T_c among the Fe-based superconductors.[16] Also, $(Sr_4Sc_2O_6)(Fe_2P_2)$ [Sc-42622(P)][12] and $(Ca_4Al_2O_6)(Fe_2P_2)$ [Al-42622(P)][18] have $T_c = 17$ K, which is the highest value among those for FeP-based superconductors.

From the structural point of view, alloying between $(Ca_4Al_2O_6)(Fe_2As_2)$ [Al-42622(As), $T_c = 28$ K] and Al-42622(P) ($T_c = 17$ K) is most intriguing. For the iron-based superconductors, there is a wide consensus that the shape of the FePn_4 tetrahedra is crucial for determining T_c, with the maximal T_c being attained when the FePn_4 tetrahedra become regular-shaped [As−Fe−As bond angle (α in Figure 1) of

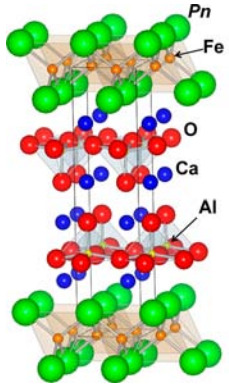

	Pn = As	*Pn* = P
T_c (K)	28.3	17.1
a (Å)	3.7133	3.6928
c (Å)	15.404	14.927
$l_{Fe\text{-}Pn}$ (Å)	2.387	2.262
$\alpha_{Pn\text{-}Fe\text{-}Pn}$ (°)	102.1	109.4
$h_{Fe\text{-}Pn}$ (Å)	1.500	1.306

Figure 1. Schematic crystal structure of $(Ca_4Al_2O_6)(Fe_2Pn_2)$. The table at the right shows the crystal structure parameters for *Pn* = As and P.

109.5°].[20] In the case of Al-42622(As), α is estimated to be 102.1°, which is the smallest value among all the existing FeAs superconductors.[18] Here the small α comes from the short *a*-axis lattice parameter (3.71 Å). This small value of α is due to the small size of the $CaAlO_3$-based perovskite block layers, which results in the elongation of the $FeAs_4$ tetrahedron along the *c* axis. On the other hand, Al-42622(P) possesses a FeP_4 tetrahedron close to the regular shape ($\alpha = 109.4°$). Accordingly, in the present system, substitution of P for As systematically should change the shape of the $FeAs_4$ tetrahedron in the direction that favors higher T_c.

On the basis of the above reasoning, we synthesized solid solutions of the Al-42622(As) and Al-42622(P) superconductors of the form $(Ca_4Al_2O_6)(Fe_2(As_{1-x}P_x)_2)$ [Al-42622-(As,P)] and characterized their physical properties. While the main purpose of this study was to establish for the first time the As−P solid-solution phase diagram, which possesses two

Received: June 8, 2012
Published: August 30, 2012

   dx.doi.org/10.1021/ja305548s | *J. Am. Chem. Soc.* 2012, 134, 15181−15184

superconducting end members, we also expected to find an enhancement of T_c in the alloyed system since it should result in tuning of the $FeAs_4$ local structure. Against the initial expectation, we instead found that the superconductivity vanished over a wide composition range from x = 0.50 to 0.95, in striking contrast to typical iron-based superconductors such as $BaFe_2(As,P)_2$ and LaFe(As,P)O, in which superconductivity shows up when P and As are alloyed.

Polycrystalline samples of Al-42622(As,P) were synthesized by the solid-state reaction method using a high-pressure (HP) synthesis technique. The starting materials (CaO, Al, As, P, Fe, and Fe_2O_3) were weighed with the corresponding compositions and mixed together using an agate mortar within a glovebox filled with dry N_2 gas. The mixed powder was loaded into a HP cell and then heated beyond 1150 to 1300 °C under an external pressure of 4.5 GPa. Details of the sample synthesis are described in ref 18. Powder X-ray diffraction (PXRD) patterns were measured with Cu Kα radiation, and direct current (dc) magnetic susceptibility was measured with a SQUID magnetometer (Quantum Design MPMS). The resistivity was measured by the four-probe method.

Figure 2 shows PXRD patterns for $(Ca_4Al_2O_6)(Fe_2(As_{1-x}P_x)_2)$ samples with x = 0.0, 0.20, 0.50, 0.75, 1.0.

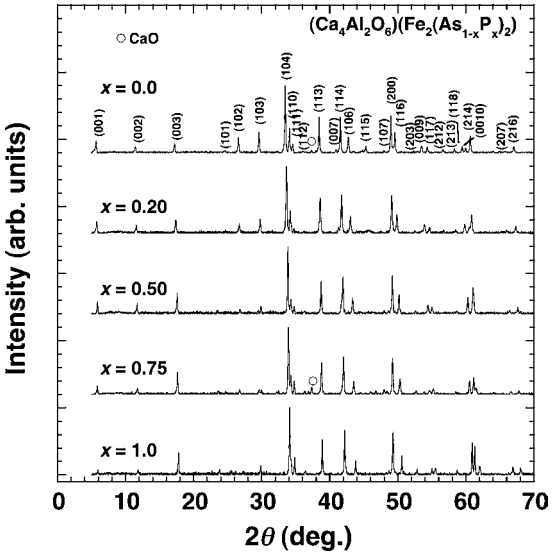

Figure 2. PXRD patterns for $(Ca_4Al_2O_6)(Fe_2(As_{1-x}P_x)_2)$ with x = 0, 0.5, 0.75, and 1.0. Peaks labeled with open circles indicate a CaO impurity phase.

Major peaks were indexed on the basis of the tetragonal crystal structure ($P4/nmm$), while a small amount of CaO was detected in some of the PXRD patterns. The a- and c-axis lattice parameters were calculated from the PXRD patterns using the least-squares method, as shown in Figure 3. The lattice parameters changed with x almost linearly, following Vegard's law. The c-axis lattice parameter of Al-42622(P) is shorter than that of Al-42622(As) by 3.1%, which is comparable to the results for LaFePnO (~2.6%)[1,21] and $BaFe_2Pn_2$ (~4.3%).[22] On the other hand, the contraction of the a-axis lattice parameter was ~0.6%, which is much smaller than those for LaFePnO (~1.8%) and $BaFe_2Pn_2$ (~2.9%) and is due to the rigid structure of the $CaAlO_3$-based perovskite-type block units. As a result, the shape of the $FePn_4$ tetrahedra changes without changing the Fe−Fe distance.

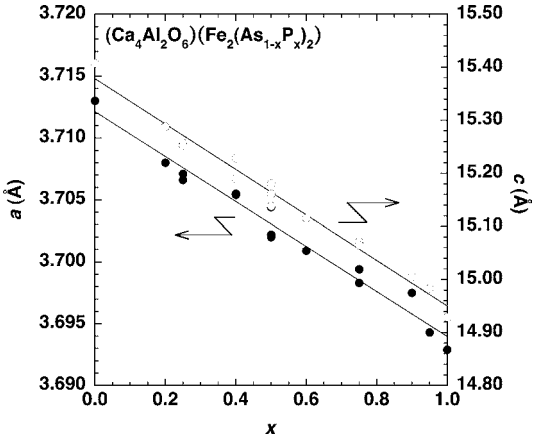

Figure 3. Lattice parameters for the a axis (●) and c axis (○) as functions of x in $(Ca_4Al_2O_6)(Fe_2(As_{1-x}P_x)_2)$.

Figure 4 shows the temperature dependence of the zero-field-cooled (ZFC) and field-cooled (FC) magnetic susceptibilities (χ) for samples with x = 0.0, 0.20, 0.50, 0.60, 0.75, 0.95, and 1.0. The samples with x = 0.0, 0.20, 0.50, and 1.0 showed clear superconducting transitions at onset temperatures of 26.8, 22.5, 4.2, and 16.9 K, respectively. T_c for the x = 0.20 sample was lower than that for the x = 0 one by 4 K. At x = 0.50, T_c exhibited salient sample dependence, ranging from 16 to <2 K, suggesting that the phase boundary between the superconducting and non-superconducting regions exists around this composition. On the other hand, for the samples with x = 0.60, 0.75, and 0.95, there was no trace of superconductivity above 2 K. Notably, the superconductivity appeared again for x

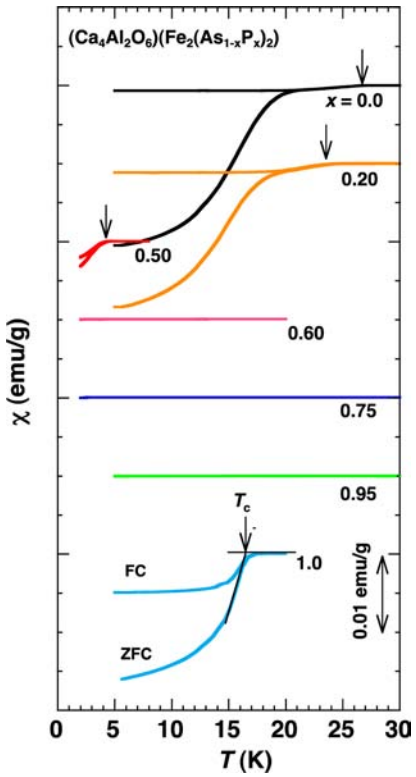

Figure 4. Temperature dependence of the magnetic susceptibility of $(Ca_4Al_2O_6)(Fe_2(As_{1-x}P_x)_2)$ with x = 0, 0.2, 0.5, 0.6, 0.75, 0.95, and 1.0. Black arrows indicate the onsets of superconducting transitions.

dx.doi.org/10.1021/ja305548s | J. Am. Chem. Soc. 2012, 134, 15181−15184

= 1.0. Near x = 1.0, a small amount of As was sufficient to suppress the superconductivity completely.

In Figure 5, T-dependent resistivity (ρ) data for the same samples are shown. The samples with x = 0.0, 0.20, 0.50, and

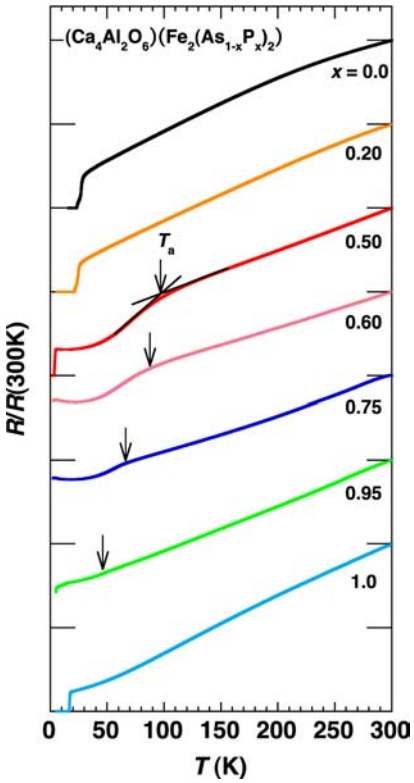

Figure 5. Temperature dependence of the resistivity of $(Ca_4Al_2O_6)(Fe_2(As_{1-x}P_x)_2)$ with x = 0, 0.2, 0.5, 0.6, 0.75, 0.95, and 1.0. Resistivity anomalies (kinks) are indicated by black arrows.

1.0 showed superconducting transitions at almost the same temperatures observed in the susceptibility measurements. There was no clear superconducting transition above 2 K for x = 0.60, 0.75, and 0.95, consistent with the susceptibility measurements. Notably, the non-superconducting and low-T_c samples (x = 0.50, 0.60, 0.75, 0.95) exhibited resistivity anomalies (kinks), which are indicated by black arrows. The kink temperature (T_a) was highest for the x = 0.50 sample (97 K) and systematically decreased with x, reaching 50 K for x = 0.95. The feature became more obscure with increasing x, finally becoming indiscernible at x = 1.0. The observed kink behavior is reminiscent of the resistivity anomaly accompanying the AFM order phase transition, which is recognized as the hallmark of the parent compounds of the FeAs-based superconductors.

On the basis of the above results, the electronic phase diagram of the Al-42622(As,P) solid-solution system is depicted as Figure 6. Here T_c and T_a were determined from the magnetic susceptibility and resistivity data, respectively. With increasing x, T_c gradually decreases up to x = 0.50, at which point the superconductivity suddenly disappears. The non-superconducting region dominates the phase diagram over a wide range from x = 0.50 to 0.95, followed by the sudden recovery of the superconductivity at x = 1.0. This phase diagram is in stark contrast to those of typical iron-based superconductors such as $BaFe_2(As,P)_2$ and LaFe(As,P)O, where the superconductivity appears upon P substitution into

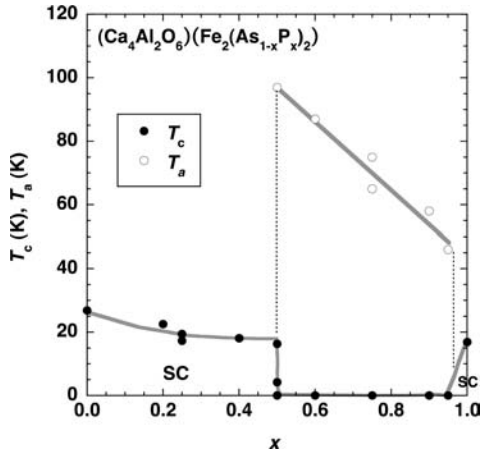

Figure 6. T_c and T_a as functions of x in $(Ca_4Al_2O_6)(Fe_2(As_{1-x}P_x)_2)$. Results not presented in Figures 4 and 5 are also plotted.

the non-superconducting parent compounds that exist around x = 0.

What is the reason for the disappearance of superconductivity from x = 0.50 to 0.95? The immediate candidate is the effect of disorder introduced by the substitution of P at random positions. However, the effect of As−P disorder is considered to be rather weak in iron-based superconductors on the basis of the following experimental facts: (1) In the solid solution between $LaFeAsO_{0.9}F_{0.1}$ (T_c = 26 K) and $LaFePO_{0.9}F_{0.1}$ (T_c = 7 K), T_c changes almost linearly with P content.[23] There is no additional decrease in T_c ascribed to the disorder effect in the intermediate region. (2) In $BaFe_2Pn_2$, superconductivity appears as a consequence of alloying. The resultant metallic state is highly conductive, as evidenced by the observation of quantum oscillations.[24] This result implies that the effect of P disorder is very weak in the $BaFe_2Pn_2$ system. We also note that the existence of the non-superconducting region in Al-42622(As,P) cannot be explained by theoretical band calculations.[25,26]

As pointed out above, the resistivity of the non-superconducting samples was characterized by the kink at 50−100 K. This is reminiscent of the behavior observed in the parent compounds, in which case it is related to the onset of the AFM long-range order. The similarity suggests that the lack of the superconductivity in the present As−P alloyed samples is also associated with the AFM order. We remark that the signature of the AFM long-range order in the alloyed samples was actually confirmed by ^{31}P-NMR measurements on the same samples.[27]

As also pointed out above, the $FeAs_4$ tetrahedra of Al-42622(As) are elongated along the c axis, resulting in the small α value of 102.1°. Notably, another "stoichiometric" FeAs-based superconductor, LiFeAs, also possesses elongated $FeAs_4$ tetrahedra with α = 103.1°.[28] In terms of the shape of the tetrahedra, these materials are distinct from other stoichiometric non-superconducting (AFM-exhibiting) compounds, such as LaFeAsO (α = 113.5°),[1] SmFeAsO (α = 110.5°),[28] $BaFe_2As_2$ (α = 111.1°),[29] NaFeAs (α = 108.6°),[30] which commonly possess α much closer to the regular value of 109.5°. The value of α is considered as a critical parameter that determines the ground state of the stoichiometric FeAs-based compounds because NaFeAs and LiFeAs possess different ground states despite the fact that they have the same crystal structure. Small (large) α favors the superconducting (AFM/orthorhombic) ground state.

dx.doi.org/10.1021/ja305548s | J. Am. Chem. Soc. 2012, 134, 15181−15184

In the case of Al-42622(As,P), P substitution for As results in squeezing of the elongated FePn_4 tetrahedra toward the regular shape. According to the aforementioned material trend, this deformation results in suppression of the superconducting ground state and favors the AFM ground state. Along this line, the disappearance of the superconductivity has a structural origin and can be ascribed to the emergence of the AFM order. If this is the case, one can naturally explain why the phase diagram of the Al-42622(As,P) system differs from those of $BaFe_2(As,P)_2$ and LaFe(As,P)O, since the latter two systems possess regular $FeAs_4$ tetrahedra in the As end members ($x = 0$) and the P substitution results in deformation of the tetrahedra away from the regular shape.

To date, regular tetrahedra have been believed to favor high T_c values. The present results suggest that in the stoichiometric compounds, regular tetrahedra also favor the AFM long-range order. This is naturally understandable, since the stronger antiferromagnetic/structural (orbital) interaction should yield a higher T_c once it contributes to the formation of Cooper pairs.

In summary, we have found that a non-superconducting region exists in the phase diagram of solid solutions between $(Ca_4Al_2O_6)(Fe_2As_2)$ and $(Ca_4Al_2O_6)(Fe_2P_2)$ superconductors. The superconductivity is strongly suppressed for a wide composition range of $0.50 < x \leq 0.95$ in $(Ca_4Al_2O_6)$-$(Fe_2(As_{1-x}P_x)_2)$. This result demonstrates again the importance of the As−Fe−As bond angle α for superconductivity in the iron pnictides. The non-superconducting and low-T_c samples have resistive anomalies over the temperature range from 46 to 97 K depending on x. We propose that the development of AFM order below T_a is a possible reason for the vanishing of the superconductivity. The Al-42622(As,P) system will provide a new platform for understanding the mechanism of superconductivity in iron-based superconductors.

AUTHOR INFORMATION

Corresponding Author

paras.shirage@gmail.com; iyo-akira@aist.go.jp

Notes

The authors declare no competing financial interest.

ACKNOWLEDGMENTS

This work was supported by a Grant-in-Aid for Specially Promoted Research (20001004) from The Ministry of Education, Culture, Sports, Science and Technology (MEXT).

REFERENCES

(1) Kamihara, Y.; Watanabe, T.; Hirano, M.; Hosono, H. *J. Am. Chem. Soc.* **2008**, *130*, 3296.

(2) Sefat, A. S.; Jin, R.; McGuire, M. A.; Sales, B. C.; Singh, D. J.; Mandrus, D. *Phys. Rev. Lett.* **2008**, *101*, No. 117004.

(3) Rotter, M.; Tagel, M; Johrendt, D. *Phys. Rev. Lett.* **2008**, *101*, No. 107006.

(4) Chen, X. H.; Wu, T.; Wu, G.; Liu, R. H.; Chen, H.; Fang, D. F. *Nature* **2008**, *453*, 761.

(5) Miyazawa, K.; Kihou, K.; Shirage, P. M.; Lee, C. H.; Kito, H.; Eisaki, H.; Iyo, A. *J. Phys. Soc. Jpn.* **2009**, *78*, No. 034712.

(6) Ren, R.-A.; Che, G. C.; Dong, X. L.; Yang, J.; Lu, W.; Yi, W.; Shen, X. L.; Li, Z. C.; Sun, L. L.; Zhou, F.; Zhao, Z. X. *Europhys. Lett.* **2008**, *83*, 17002.

(7) Wang, Z. W.; Yang, H. X.; Ma, C.; Tian, H. F.; Shi, H. L.; Lu, J. B.; Zeng, L. J.; Li, J. Q. *J. Phys.: Condens. Matter* **2009**, *21*, No. 495701.

(8) Colombier, E.; Bud'ko, S. L.; Ni, N.; Canfield, P. C. *Phys. Rev. B* **2009**, *79*, No. 224518.

(9) Wang, C.; Jiang, S.; Tao, Q.; Ren, Z.; Li, Y.; Li, L.; Feng, C.; Dai, J.; Cao, G.; Xu, Z.-A *Europhys. Lett.* **2009**, *86*, 47002.

(10) Takeshita, N.; Yamazaki, T.; Iyo, A.; Eisaki, H.; Kito, H.; Ito, T.; Hirayama, K.; Fukazawa, H.; Kohori, Y. *J. Phys. Soc. Jpn.* **2008**, *77* (Suppl. C), 131−133.

(11) Wang, X. C.; Liu, Q. Q.; Lv, Y. X.; Gao, W. B.; Yang, L. X.; Yu, R. C.; Li, F. Y.; Jin, C. Q. *Solid State Commun.* **2008**, *148*, 538.

(12) Ogino, H.; Matsumura, Y.; Katsura, Y.; Ushiyama, K.; Horii, S.; Kishio, K.; Shimoyama, J. *Supercond. Sci. Technol.* **2009**, *22*, No. 075008.

(13) Zhu, X.; Han, F.; Mu, G.; Cheng, P.; Shen, B.; Zheng, B.; Wen, H. H. *Phys. Rev. B* **2009**, *79*, No. 220512(R).

(14) Sato, S.; Ogino, H.; Kawaguchi, N.; Katsura, Y.; Kishio, K.; Shimoyama, J. *Supercond. Sci. Technol.* **2010**, *23*, No. 045001.

(15) Ogino, H.; Sato, S.; Kishio, K.; Shimoyama, J.; Tohei, T.; Ikuhara, Y. *Appl. Phys. Lett.* **2010**, *97*, No. 072506.

(16) Ogino, H.; Shimizu, Y.; Ushiyama, K.; Kawaguchi, N.; Kishio, K.; Shimoyama, J. *Appl. Phys. Express* **2010**, *3*, No. 063103.

(17) Ogino, H.; Machida, K.; Yamamoto, A.; Kishio, K.; Shimoyama, J.; Tohei, T.; Ikuhara, Y. *Supercond. Sci. Technol.* **2010**, *23*, No. 115005.

(18) Shirage, P. M.; Kihou, K.; Lee, C. H.; Kito, H.; Eisaki, H.; Iyo, A. *Appl. Phys. Lett.* **2010**, *97*, No. 172506.

(19) Shirage, P. M.; Kihou, K.; Lee, C. H.; Kito, H.; Eisaki, H.; Iyo, A. *J. Am. Chem. Soc.* **2011**, *133*, 9630.

(20) Lee, C. H.; Iyo, A.; Eisaki, H.; Kito, H.; Fernandez-Diaz, M. T.; Ito, T.; Kihou, K.; Matsuhata, H.; Braden, M.; Yamada, K. *J. Phys. Soc. Jpn.* **2008**, *77*, No. 083704.

(21) Kamihara, Y.; Hiramatsu, H.; Hirano, M.; Kawamura, R.; Yanagi, H.; Kamiya, T.; Hosono, H. *J. Am. Chem. Soc.* **2006**, *128*, 10012.

(22) Jiang, S.; Xing, H.; Xuan, G.; Wang, C.; Ren, Z.; Feng, C.; Dai, J.; Xu, Z.; Cao, G. *J. Phys.: Condens. Matter* **2009**, *21*, No. 382203.

(23) Miyasaka, S.; Suzuki, S.; Saijo, S.; Mikasa, Y.; Matsui, T.; Tajima, S. *J. Phys.: Conf. Ser.* **2009**, *150*, No. 052164.

(24) Analytis, J. G.; Chu, J.-H.; McDonald, R. D.; Riggs, S. C.; Fisher, I. R. *Phys. Rev. Lett.* **2010**, *105*, No. 207004.

(25) Miyake, T.; Kosugi, T.; Ishibashi, S.; Terakura, K. *J. Phys. Soc. Jpn.* **2010**, *79*, No. 123713.

(26) Although P and As are isovalent (3+), carriers induced by the substitution of P for As cannot be ruled out as a possible reason for the disappearance of superconductivity . See: Ye, Z. R.; Zhang, Y.; Xu, M.; Ge, Q. Q.; Chen, F.; Jian, J.; Xie, P. B., Hu, J. P.; Feng, D. L. 2011, arXiv:1105.5242V1. arXiv.org e-Print archive (accessed June 8, 2012).

(27) Kinouchi, H.; Mukuda, H.; Kitaoka, Y.; Shirage, P. M.; Eisaki, H., Iyo, Y. 2012, arXiv:1207.1920v1. arXiv.org e-Print archive (accessed June 8, 2012).

(28) Martinelli, A.; Ferretti, M.; Manfrinetti, P.; Palenzona, A.; Tropeano, M.; Cimberle, M. R.; Ferdeghini, C.; Valle, R.; Bernini, C.; Putti, M.; Siri, A. S. *Supercond. Sci. Technol.* **2008**, *21*, No. 095017.

(29) Rotter, M.; Tegel, M.; Johrendt, D.; Schellenberg, I.; Hermes, W.; Pöttgen, R. *Phys. Rev. B* **2008**, *78*, No. 020503(R).

(30) Li, S.; de la Cruz, C.; Huang, Q.; Chen, G. F.; Xia, T.-L.; Luo, J. L.; Wang, N. L.; Dai, P. *Phys. Rev. B* **2009**, *80*, No. 020504(R).